

# Myelin and myelination in the telencephalon and mesencephalon of the lizard *Gallotia galloti* as revealed by the immunohistochemical localization of myelin basic protein

C. Yanes<sup>1</sup>, M. Monzon-Mayor<sup>2</sup>, J. de Barry<sup>3</sup>, and G. Gombos<sup>3</sup>

<sup>1</sup> Departamento de M. y Biología Celular, Facultad de Biología, Universidad de La Laguna, Tenerife, Canary Islands, Spain

<sup>2</sup> Departamento de Morfología, Facultad de Ciencias Médicas y de la Salud, Universidad de Las Palmas de G.C., Canary Islands, Spain

<sup>3</sup> Centre de Neurochimie du C.N.R.S., 5, Rue Blaise Pascal, F-67084 Strasbourg, France

Accepted December 2, 1991

**Summary.** We have studied in the telencephalon and mesencephalon of the lizard *Gallotia galloti* the localization and the chronology of appearance of the immunoreactivity due to the presence of a myelin-specific protein: the Myelin Basic Protein (MBP). MBP-like immunoreactivity was present with different degrees of intensity in many nerve fibers (isolated, in tracts and in commissurae) and it was apparently more abundant in mesencephalon. During ontogeny the earliest MBP-like immunoreactivity was detected at E.36 in few tracts in mesencephalon and appeared at E.40 in telencephalon, proceeding caudo-rostrally and from the ventral (basal) to the dorsal (alar) regions. Accumulation of MBP continued after hatching. Oligodendrocyte cell bodies were not immunopositive, not even at the youngest ages studied.

**Key words:** Cortex – Basal nuclei – Mesencephalic nuclei – Ontogenesis – Phylogenesis – Reptiles

## Introduction

Immunohistochemistry with specific antisera is one of the most clear means for localizing a protein in a tissue in which the cellular morphologic characteristics are conserved. Thus myelinated nerve tracts can be detected, and myelination can be followed, by using an antibody directed against myelin basic protein (MBP), a myelin-specific protein present in both central and peripheral nervous system (CNS and PNS respectively), (Matthieu et al. 1973; Sternberger et al. 1978a, b; Eng and Bigbee 1978). In addition, in many species, MBP has also been transiently detected, during myelination, in young oligodendrocyte cell bodies (Matthieu et al. 1973; Sternberger et al. 1978a, b; Eng and Bigbee 1978) and, in this way, oligodendrocyte formation was followed (Campagnoni et al. 1989). Many papers have been published on the identification and/or localization of MBP in the CNS,

particularly in mammals, amphibians and birds (Mendel and Withaker 1978; Hartman et al. 1979; Norton 1981; Nussbaum and Roussel 1983) but not in reptiles. In the present paper we describe an immunohistochemical study on the localization of MBP in the telencephalon and midbrain of the lizard *Gallotia galloti* during ontogenesis. This study on myelinogenesis continues our studies on gliogenesis in the cerebrum of this reptile. We have already reported on the presence and on the ultrastructure of oligodendrocytes during ontogeny and in the adult (Monzon-Mayor et al. 1990d) and, by using cell specific antibodies, we have shown the distribution and the development of astrocytes and radial glia in this lizard (Monzon-Mayor et al. 1990a–d; Yanes et al. 1990).

## Materials and methods

**Antibodies.** The rabbit polyclonal antibody directed against bovine MBP (Chemicon, Calif., USA) was raised and kindly given to us by Dr M.S. Ghandour. The goat antirabbit immunoserum and rabbit peroxidase antiperoxidase (PAP) complex were purchased from Sternberger and Meyer (Jarrettsville, Md., USA). All other chemicals were of analytical grade.

**Animals and tissue fixation.** *Gallotia galloti* (Bischoff 1982) (family: *Lacertidae*; order: *Squamata*) is a lizard indigenous to the island of Tenerife. We used a large number of these lizards of different ages (from embryonic stage 32 to adults). The stages of embryonic development were defined according to the tables of equivalence between the development of the *Gallotia galloti* (Ramos 1980) and of *Lacerta vivipara* (Dufaure and Hubert 1961).

Embryos and very young lizards were decapitated, and their heads immersed for about 2 days in the fixative [2% paraformaldehyde and 0,25% glutaraldehyde in PBS (0.15 M NaCl in 0.1 M phosphate buffer, pH 7.2)] while the central nervous system of adults was fixed in situ by intracardiac perfusion with the same fixative. The skull was then opened and telencephalon and brainstem were excised, cleaned from meninges and then immersed for 3 to 4 h in the same fixative.

Handling of the embryo sections were very difficult due to their small size, hence the encephalon and brainstem of embryos and young animals were embedded in 4% agarose before slicing into

sections 50 to 100  $\mu\text{m}$  thick with a Vibratome (Oxford instrument, Foster city, USA). Sections were kept at  $+4^\circ\text{C}$  until processed as described below.

**Immunohistochemistry.** All incubations were carried out at room temperature unless otherwise specified. Antibodies were diluted in TBS (0.15 M NaCl in Tris HCl pH 7.4) which contained 0.5% BSA, and after each step the sections were washed three times (10–15 min each time) in 0.5% BSA in TBS. Free floating sections were at first permeabilized with ethanol-acetic acid (95:5, v/v) at  $-20^\circ\text{C}$  for 10 min, then preincubated for 1 h in small Petri dishes containing 4% BSA in PBS, then another hour in 0.1 M glycine, and finally incubated overnight either with the primary antibody or, for control, with non-immune rabbit serum (both diluted 1:250 in PBS containing 0.01%  $\text{NaN}_3$  and 1:100 normal sheep serum). Next day, the sections were incubated for 30 min with goat antirabbit immunoserum (1/80) and then with the PAP complex as described by Sternberger et al. (1970). The peroxidase activity was revealed with diaminobenzidine (DAB) according to the method of Graham and Karnovsky (1966). Microscopic observations were carried out as previously described (Ghandour et al. 1983).

**Antiserum specificity.** Antiserum specificity was verified by western blot. Briefly, adult *Gallotia galloti* brain homogenates or rat myelin extracts in sodium dodecyl sulfate (SDS) were electrophoresed on polyacrylamide gel (7.5%) in the presence of SDS. The electrophoretic pattern was then electrotransferred on a cellulose nitrate membrane (HAWP, Millipore France, Molsheim, France) and immunoreactive bands were revealed by the PAP method as described above. Using this procedure the immune serum revealed a single band of 19 kD in the lizard brain homogenate electrophoregram, while in the rat three bands (17 kD major, 19 kD, and a minor band of 20 kD) were revealed. This is in close agreement with the multiple MBP molecular weight forms reported by all the authors in rat central nervous system, with the single 18.5 kD electrophoretic band previously described by Waehnelde et al. (1986) for another reptile (python) and with the predominant 18.5 kD electrophoretic band described by Matthieu et al. (1986) for lizard. We did not detect however the very minor 14 kD component observed in electrophoregrams of purified lizard myelin extracts (Matthieu et al. 1986) but in any case only MBP and no other protein of a different molecular weight was recognized by the antiserum used by us.

## Results

At all ages examined, we never detected any immunostaining in cell bodies, indeed only fibers appeared to be immunopositive.

### Adult telencephalon

Immunoreactivity to an antiserum recognizing MBP was studied on sections of the lizard cerebrum cut as shown in Fig. 1 for the adult.

In the adult telencephalon, MBP immunoreactivity was present and strong in well defined tracts (Fig. 2). Some MBP-positive fiber systems appeared to be cross sectioned; this was the case of the medial (mfb) and of the lateral (lfb) forebrain bundles which run ventrally to the ventral striatum (Stv) (Fig. 2a, b) and to the anterior dorsal ventricular ridge (ADVR) (Fig. 2c). Some of the lfb fibers crossing the Strv, (Figs. 2b, 3b) and the nucleus centralis amygdalae (Amc) (Figs. 2c, 3d) were obliquely sectioned. Another system of immunore-

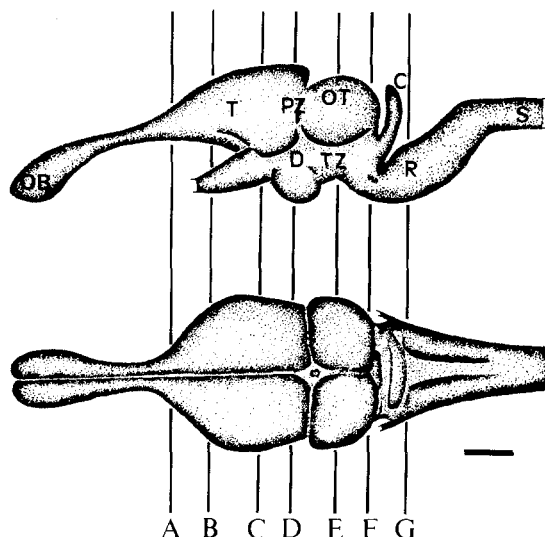


**Fig. 1.** Drawing of the brain of the lizard *Gallotia galloti* CNS showing the approximate level of the sections shown in this paper. OB, olfactory bulb; T, telencephalon; D, diencephalon; PT, pretectal zone; TZ, tegmental zone; OT, optic tectum; C, cerebellum; R, rhombencephalon; S, spinal cord. Distance in  $\mu\text{m}$  from the stria medullaris: A +2610; B +2220; C +850; D 000; E -1720; F -2,330; G -2,960. Bar 2 mm

active fibers was that of the tractus olfactorius lateralis (tolf) which delimits ventrally and laterally the Strv and the nucleus tracti olfactorii lateralis (Ntol) (Figs. 2b, 3e) and the nucleus sphericus (NS) (Figs. 2d, 3h).

In the septum, cross- and obliquely-sectioned MBP-positive fibers were detected; these were the fibers of the septo-hypothalamic tract (tsh) running near the nucleus septalis anterior (Nsa) (Figs. 2a–c, 3c) and of the tractus paraolfactorius corticalis (tpoc) which begins rostrally to the Nsa (Figs. 2b, c, 3c) and runs ventrally to it.

In the areas corresponding to the commissura anterior (ca) only a few weakly immunoreactive fibers were detected (Figs. 2c, 3f), this is due to limited myelination, as indicated by classical myelin-specific histological techniques such as the Klüver-Barrera (not shown). By contrast tightly-packed, strongly-immunoreactive fibers were present in the commissura pallii anterior (cpa) (Figs. 2c, 3f).

The alveus (alv) exhibited MBP-positive fibers which course in the plane of the section apparently emerging from the dorsal region of the nucleus septalis lateralis (Nsl) (Fig. 2b–d). In the subcortical region, these fibers then follow a path parallel to the dorsal ventricular edge in the section and finally reach the medial (MC) (Fig. 2a–d) and dorso-medial (DMC) cortex (Fig. 2d). In the medial cortex (MC) other systems of MBP-positive fibers were observed: these fibers course in the plane of the tissue section following paths similar to that of the alveus. They constitute the external (epf) and the internal (ipf) plexiform layers (Fig. 3g). In contrast immunoreactive fibers in the granular layer (gl) of the cortex run, in the tissue section, perpendicular to the dorsal edge of the ventricle. The distribution of MBP-positive fibers, particularly those of the ipf, in the DMC and

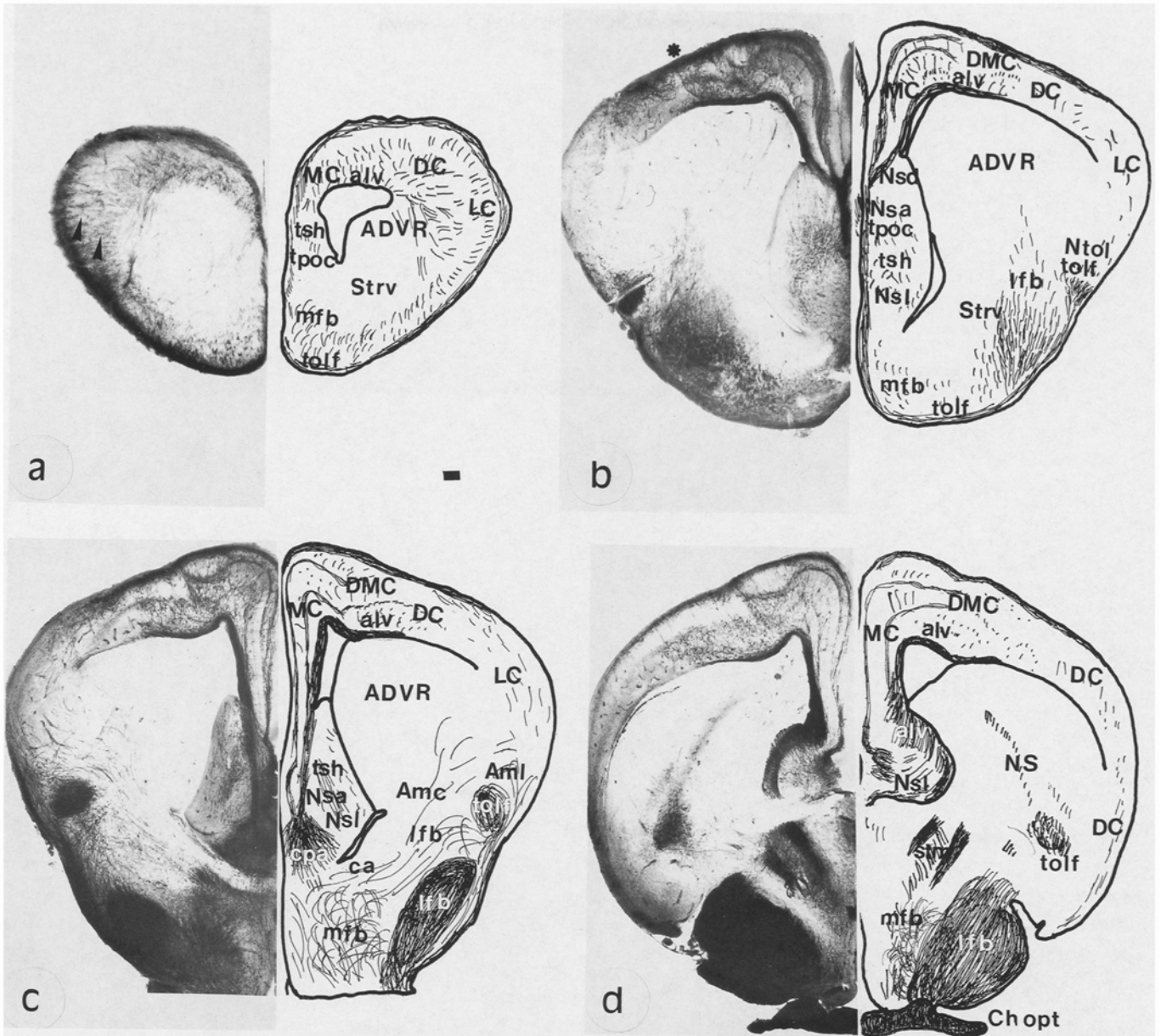


**Fig. 2a–d.** Immunohistochemical localization of MBP in four cross sections of the adult telencephalon. The sections are arranged in a rostro-caudal sequence from *A* to *D* corresponding to the levels indicated in Fig. 1. The *left half* of each section shows the immunoreactivity, and the *right half* schematically illustrates the nerve fibers, the nuclei and the cortex in the section. Bar 200  $\mu$ m. **a** Most rostral level (corresponds to level *A* in Fig. 1). Intense and compact immunolabel is localized in the following cross-sectioned tracts: medial forebrain bundle (*mfb*), tractus septo-hypothalamicus (*tsh*), tractus paraolfactorius corticalis (*tpoc*), and tractus olfactorius (*tolf*). Also strongly labeled are tangentially sectioned bundles like the alveus (*alv*) and tangential fiber in the inner layers of the lateral anterior cortex (*LC*) where they form radial columns (*arrow head*). Other labeled fibers run in the plane of the section under the pial surface of the *LC* and of the medial cortex (*MC*). **b** Anterior level (corresponds to level *B* in Fig. 1). The same cross-sectioned tracts seen in the previous sections (*mfb*, *tsh*, *tolf*), the *alv* and new tracts like the lateral forebrain bundle (*lfb*) are labeled.

In the cortex, the label is concentrated at the level of the plexiform layer of the medial cortex (*MC*) and it is more superficial in the dorsal cortex (*DC*) where it corresponds to the tangential fiber layer (Molowny et al. 1972) but is virtually absent in the lateral cortex (*LC*). The *ADVR* and the striatum ventralis (*Strv*) are crossed by tangentially cut immunopositive fibers. **c** Intermediate level (corresponds to level *C* in Fig. 1). The commissura anterior (*ca*) and the commissura pallii anterior (*cpa*) appear to be labeled in addition to the previously mentioned fiber bundles (*mfb*, *lfb*, *tsh*, *tolf*, *alv*). The immunolabel pattern in the cortex is similar to that observed in more rostral section. The amygdala central nucleus (*Amc*) is crossed by the tangentially cut immunopositive fibers of the *lfb*. **d** Caudal level (corresponds to level *D* in Fig. 1). The *alv* and *mfb* are still labeled while *ca* become undetectable, and the labeled stria medullaris (*stm*) appears. The pattern of MBP-positive fibers in the cortex is similar to that observed in more rostral sections

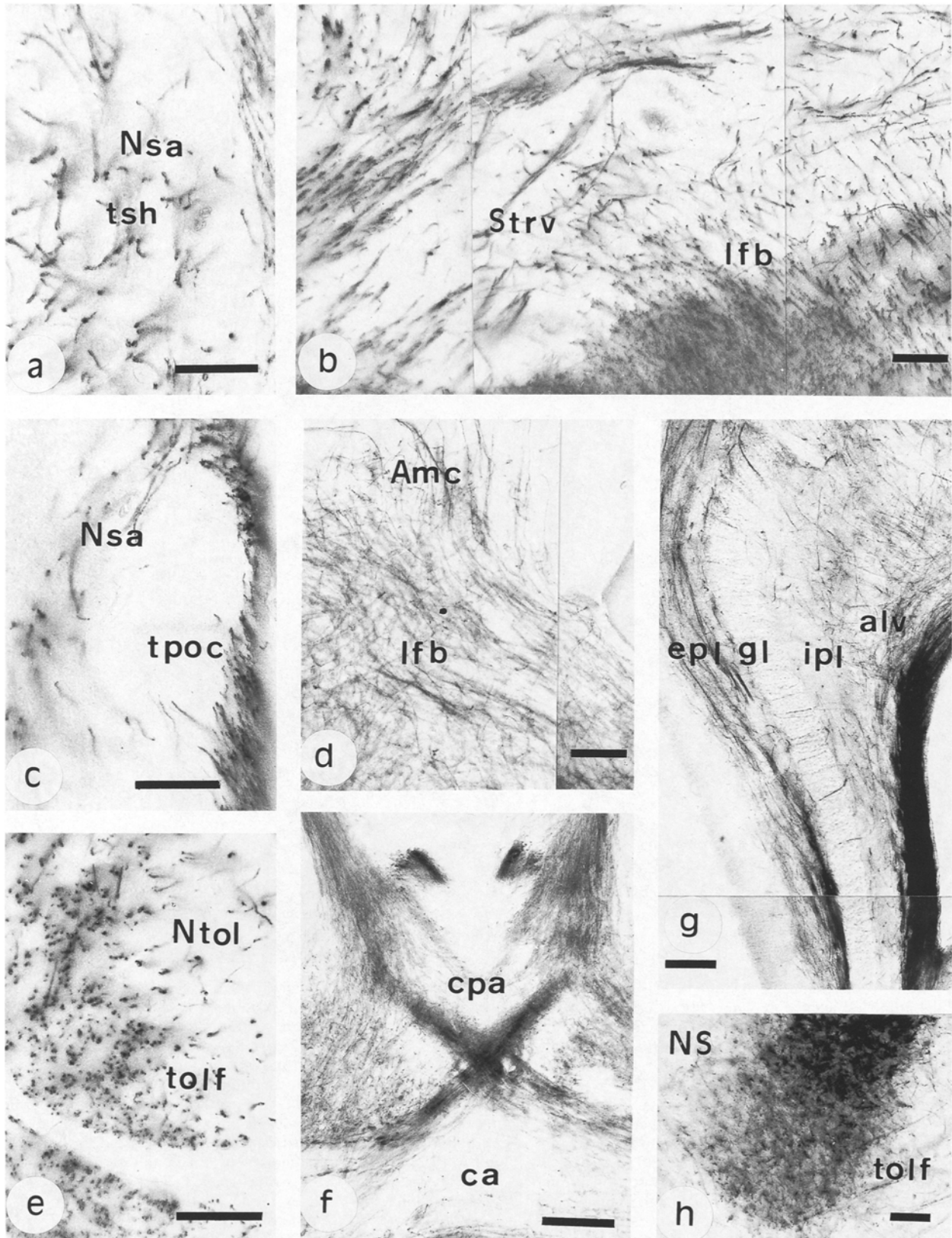


**Fig. 3a–h.** Details at higher magnification of the cross sections of adult telencephalon shown above. Bar 100  $\mu\text{m}$  from **a** to **e**. **a** Rostral level: details of myelinated fibers in the tractus septo-hypothalamicus (*tsh*) crossing the nucleus septalis anterior (*Nsa*). **b** Anterior level: note the intense MBP-immunoreactivity in the fibers of the lateral forebrain bundle (*lfb*) invading the ventral striatum (*Strv*). **c** Rostral level: note the distribution of MBP immunoreactivity in the fibers of the tractus paraolfactorius corticalis (*tpoc*). **d** Intermediate level: immunoreactive fibers in the *lfb* cross-

ing the nucleus centralis amigdalae (*Amc*). **e** Anterior level: MBP presence in cross-sectioned fibers of the *tolf* in the nucleus of the tractus olfactorius lateralis (*Ntol*). **f** Immunoreactive fibers in the commissura pallii anterior (*cpa*). **g** Positive fibers in the alveus (*alv*), in the internal (*ipl*) and external (*epl*) plexiform layers and in the granular layer (*gl*). Bar 200  $\mu\text{m}$ . **h** Caudal level: Immunoreactive cross- and tangentially-sectioned fibers in the tractus olfactorius (*tolf*) and in the nucleus sphericus (*NS*). Bar 200  $\mu\text{m}$

in the dorsal cortex (DC) (Fig. 3g), is similar to that in the MC. In the lateral cortex (LC) immunopositive fibers were numerous and followed many different paths (Fig. 2a–c).

#### *Adult mesencephalon*

In the adult mesencephalon many more nerve tracts were immunoreactive than in the adult telencephalon. The major MBP-positive longitudinal tract was the fasciculus longitudinalis medialis (flm) (Figs. 4a, b, 5a, c, e) which goes from the anterior to the caudal end of the midbrain running along the surface of the nuclei of the III and IV nerves.

Also immunoreactive are the tractus tecto-thalamicus dorso medialis anterior (ttd) and ventrolateralis (ttv) (Fig. 4a), the tractus opticus lateralis (tol) (Fig. 4a, b, d), marginalis (tom) and basalis (tob) (Fig. 4a, b), the tractus tecto-tegmentalis (ttt) and profundus mesencephalicus (tmp) (Fig. 4b). Among the tracti tecto-bulbares are MBP-positive the ventralis rectus (tbv) (Fig. 4a, b) and the intermedius rectus (tbi) which run across the deep nuclei (Figs. 4a, b, 5a, e), the tractus tecto-bulbo-spinalis rectus (tbs) which runs at the border of the nuclei of the torus semicircularis (TS) (Fig. 4a, b), the dorsalis rectus (tbd) (Figs. 4b, 5a, e) near the oculomotor nuclei, and finally the dorsalis cruciatus (tbc) (Figs. 4b, 5a, e) which crosses the red nucleus (Rub) (Fig. 4b).

In the tectum the MBP immunoreactivity clearly defined the six typical strata described by Huber and Crosby (1933a, b; 1934): s. album periventriculare (SAP), s. griseum periventriculare (SGP), s. album centrale (SAC), s. griseum centrale (SGS), s. fibrosus and griseum superficiale (SFGS) and s. opticum (SO) (Fig. 4a, b, f). Similarly the 14 layers described by Ramon (1896) can be distinguished (Fig. 4a, b, f). At the median border of the SGP the trigeminal nucleus (nV) is located (Fig. 4a, b).

The cranial nerves are intensely immunolabeled as can be seen for the oculomotor nerve (III) (Fig. 4c) emerging from its nucleus (nIII) situated between the red nucleus and the interpeduncular nuclei (Ip) (not shown). The trochlear nerve (IV) is also intensely immunoreactive (Fig. 4e). Its nucleus (nIV) is located laterally to the isthmic nuclei (Ic and Isp) (Fig. 5e).

All commissural tracts are positive, i.e., the commissura dorsalis tegmentalis (cdt) between oculomotor and interpeduncular nuclei (Figs. 4a, b; 5a, c) and the commissura colliculi (cc) near the colliculi inferiores (Fig. 5a–d).

In caudal mesencephalic sections MBP-positive fibers are those of the lemniscus lateralis (ll) (Fig. 5a, b) crossing the isthmic nuclei and of the lemniscus medialis (lm) (Fig. 5a) located below the reticular nuclei. A fine network of positive fibers criss-crosses the corpus quadrigeminus posterior (ccp) (Fig. 5a, c) while in the commissura colliculi (cc) and in the tti MBP-positive fibers are more dense (Fig. 5a, b, d). Other immunoreactive tracts are the tractus mesencephalicus trigemini (tmt)

(Fig. 5a, b) and the more ventrally located tracti tecto-bulbaris, namely the intermedius (tbi), the dorsalis (tbd) and the cruciatus (tbc).

#### *Telencephalon during prenatal development*

During the embryonic development of the lizard no MBP-immunoreactivity was detected until stage E.32. At E.40 few positive fibers were detected in the lfb at the caudal and intermediate levels of telencephalon (not shown), but in the optic chiasma packets of strongly immunoreactive fibers were already apparent; the intensity of their immunoreactivity increased until hatching (Fig. 6b).

#### *Telencephalon during postnatal development*

During the postnatal development other fiber systems became positive. At postnatal day 5 the lfb at the anterior levels of telencephalon contained a few weakly positive fibers spreading in all directions (Fig. 6d) while the same bundle at more caudal levels displayed numerous and strongly immunoreactive fibers (Fig. 6c, e). At this same level only weakly positive fibers are detected in the dorsal cortex (Fig. 6c). Starting from postnatal day 15, the immunoreactivity increases until the pattern described for the adult is attained.

#### *Mesencephalon during prenatal development*

At E.36 only the flm (in the basal plate), the tractus mesencephalicus trigemini (tmt) and the stratum album centrale (SAC) in the alar mesencephalon are weakly immunostained (not shown).

At E.37 the immunoreactivity increases in the flm, tmt, SAC and SO and appears in the SFGS and cc (Fig. 7a, c). Tracti in the tegmentum and basal zone also begin to display immunolabeling in some fibers, i.e., fibers of the tbs, of the msp and of the tob (Fig. 7a, c), of the tol (Fig. 7a), III nerve, cdt, ttt, tmp, tbi, tbd. By contrast a greater density of MBP-positive fibers is detected in the tbc, although at caudal levels this tractus is weakly immunoreactive (not shown). The most intensely labeled tracts are the flm, the SAC and the nerve bundles in the basal pretectal region such as the tgp, the tgd, the ttd and the ttv (Fig. 7a, c).

At E.40 the different tectal layers are immunoreactive, especially the layers 9 and 12 (Fig. 7b). The immunoreactivity of all the above described tracti in the tegmentum increases, particularly in the ttt, tmp, tbi and tbd (Fig. 7b). At more caudal levels the immunoreactivity begins to appear in the ll, lm, tti, tst and tsc (not shown). Thus at E.40, as at E.37, MBP-positive structures are more abundant in the tegmentum than in the tectum.

At hatching the immunoreactivity of all the structures described above is more intense than at younger ages, particularly in the flm and in the III and IV nerves (Fig. 7d, e) as well as in the cdt (Fig. 7d). Also the immu-

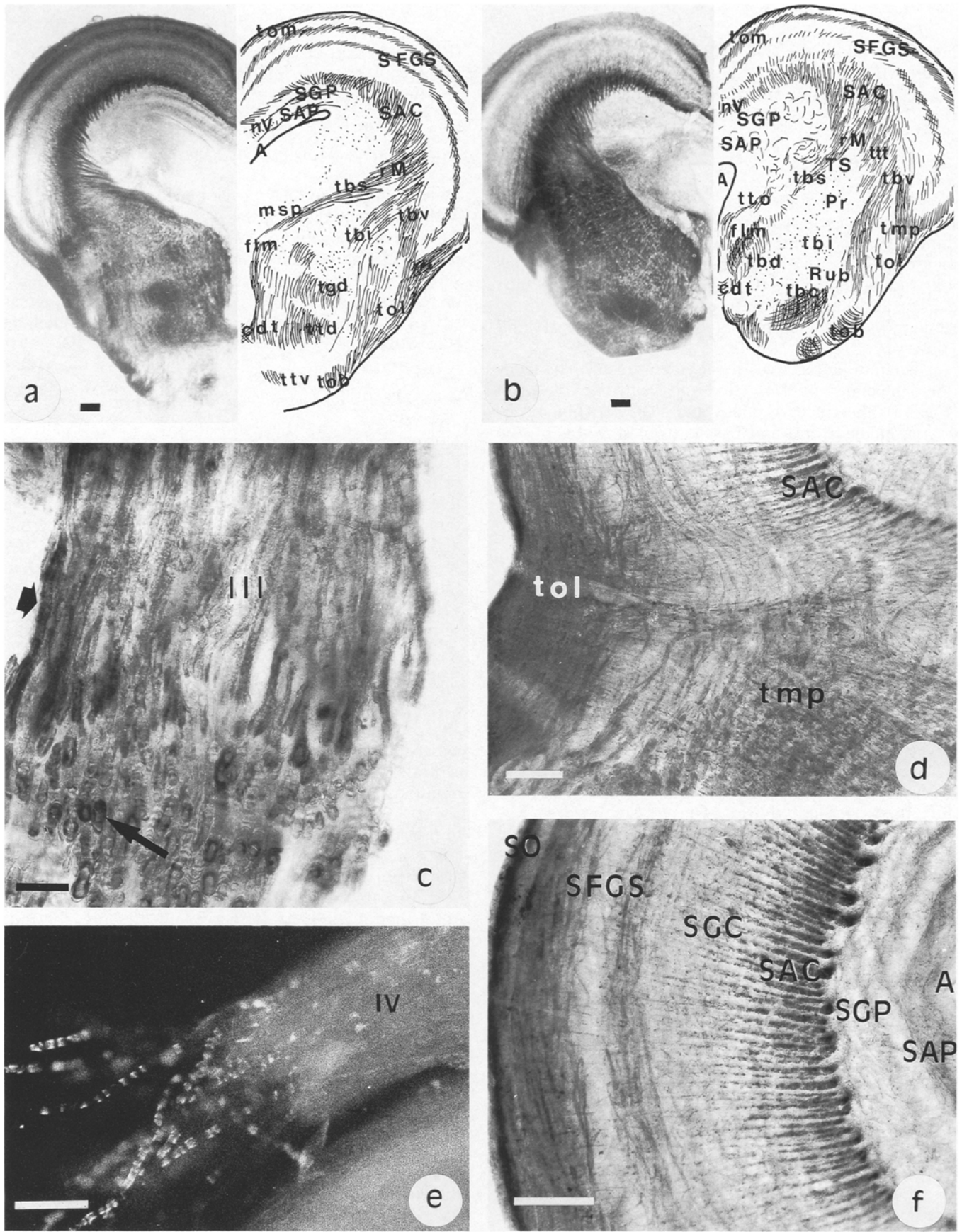


**Fig. 4a-f.** MBP-immunopositive fibers in cross-sections of pre-tectum and mesencephalon in adult lizards demonstrated by the PAP or the immunofluorescence method (for **a, b, d,** and **f** Bar 200  $\mu$ m; for **c** and **e** Bar 50  $\mu$ m). Half sections as in Fig. 2. **a** Section at the medial pretectal level (approximately between levels *D* and *E* in Fig. 1). Note the clearly defined immunopositive fiber layers

in the tectum also shown in greater detail in **f**. **b** Section at the medial mesencephalic level (approximately level *F* in Fig. 1). **c** Higher magnification of a section at the level of the oculomotor nerve (*III*) showing longitudinally sectioned immunopositive fibers (*short bold arrow*) and immunopositive rings around cross-sectioned nerve fibers (*thin long arrow*). **d** Detail at high magnification

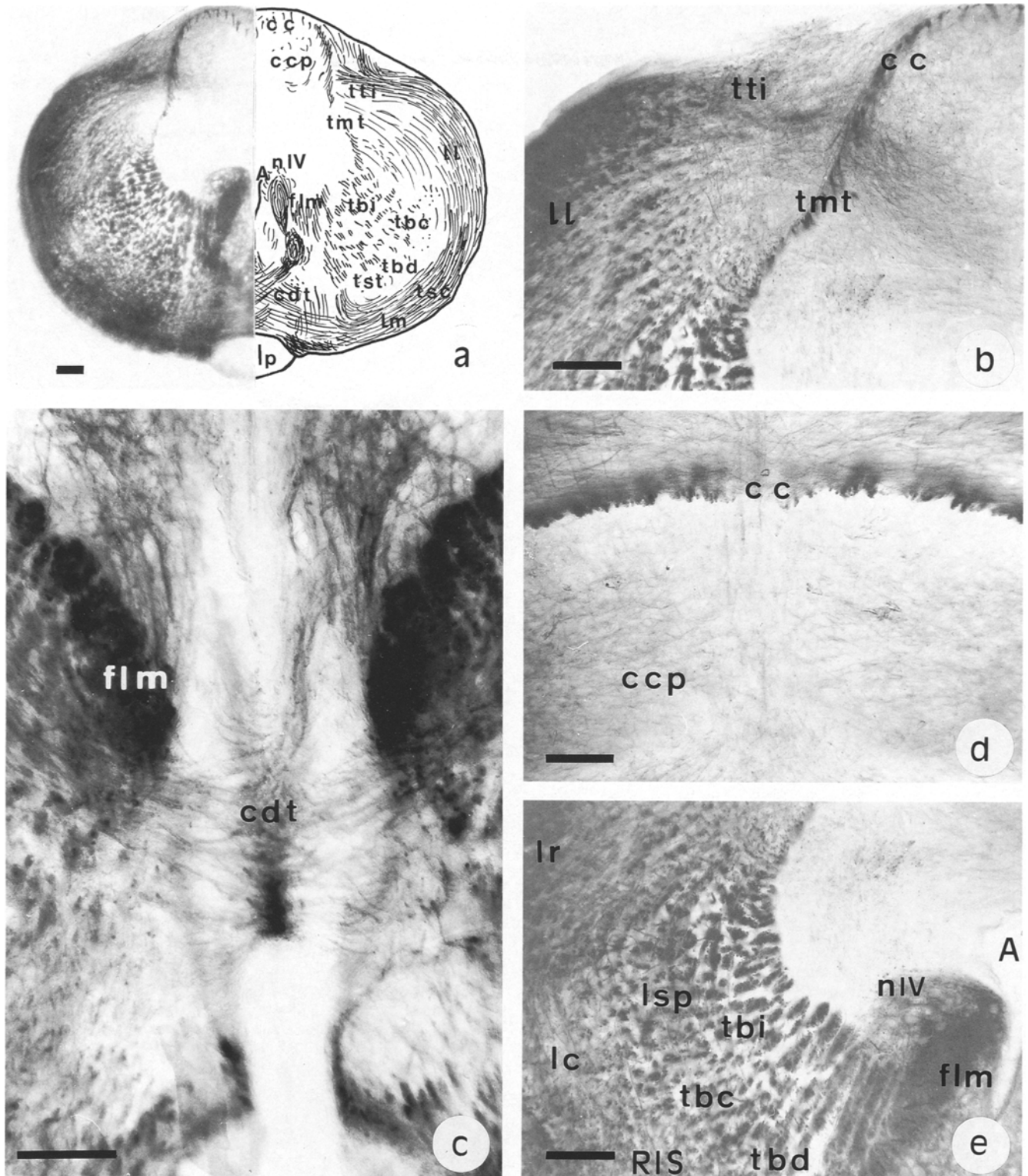


**Fig. 5a-e.** MBP-immunopositive fibers in a caudal cross section of mesencephalon in an adult lizard at approximately half way between levels *F* and *G* in Fig. 1. Bar 200  $\mu$ m. **a** Overall view at low magnification. **b**, **c**, and **e**, details of the same (or of contiguous) tissue section(s) observed at higher magnification. Notice the intense immunostain in the cross-sectioned flm (**a**, **c**, and **e**), *tbc*,

*tbd*, *tbi* (**a** and **e**). Other immunoreactive fibers coursing, at least partially, in the plane of the section are those of the *cc* (**a**, **b** and **d**), *tmt*, *tti* and *ll* (**a** and **b**), *lm* (**a**) and *cdt* (**a** and **c**) in the basal area. Notice the fine network of weakly reactive fibers in the *ccp* (**a** and **d**)

of a zone in the mesencephalon (left antero-lateral) at the same level as in **b** showing the tractus opticus lateralis (*tol*), the stratum album centrale (*SAC*) and the tractus mesencephalicus profundus (*tmp*). **e** Immunofluorescence in trochlear nerve (IV) fibers. Note that this immunofluorescence is discontinuous, the non-fluorescent bands probably corresponding to nodes of Ranvier. **f** Detail of

the tectum at high magnification of a section at the same level as in **a** showing the MBP-positive fiber "bands" in the six strata defined by Huber and Crosby (1933a, b 1934). Immunolabeled columns in *SAC* and *SAC* are made of cross-sectioned fiber bundles

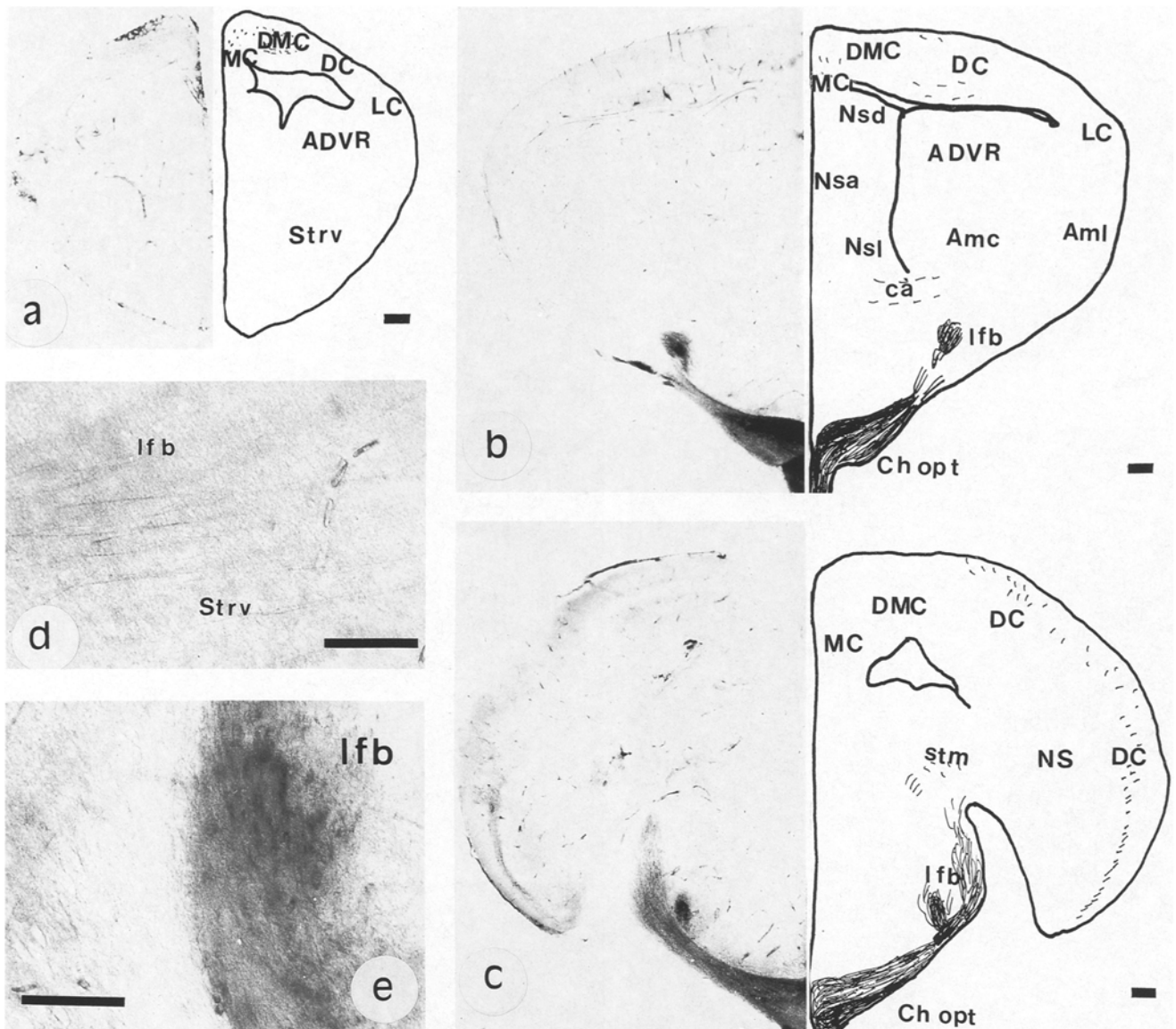


**Fig. 6a–c.** Immunohistochemical localization of MBP in cross sections of developing telencephalon. Bar 200  $\mu\text{m}$  for **a**, **b** and **c**, and 100  $\mu\text{m}$  for **d** and **e**. **a** Anterior level at E.37. The medial, dorsomedial and dorsal cortex is labeled. **b** Mid-telencephalon section at hatching: a positive immunoreaction is detected in the *lfb* and in the optic chiasma (*Ch opt*). In the medial and dorsal cortex a layer of tangential submeningeal fibers is immunopositive. **c** Cau-

dal section of telencephalon at postnatal day 15; also at this age only the *lfb* and the *Ch opt* are labeled. Superficial fibers in the dorsal cortex and the *stm* are weakly positive. **d** Detail of a section at anterior level at postnatal day 15; note the individual positive fibers which do not exhibit a preferential direction. **e** Caudal level: detail at great magnification of the *lfb* shown in **c**

noreactivity of *ll*, *lm*, *tti*, *tst* and *tsc* increases, but in this case the postnatal increase is very important.

#### Mesencephalon during postnatal development

The MBP-positive layers in the tectum become more intensely immunopositive. The same is true for all the above described tracts, fascicles and nerves of the pretectal zone and tegmentum. More precisely the *flm* (Fig. 8a, c–e), the *tmt* (Fig. 8a, b), and the SAC (not shown) which are the earliest to be formed are also the most intensely immunolabeled; the other fibers are those of

**Fig. 7a–e.** Immunopositive fibers in pretectal and mesencephalic cross sections in lizards at E.37, E.40 and at hatching. Bar 200  $\mu\text{m}$ . **a** Section at the rostral pretectal level at E.37, note the weak immunopositivity of the nerve fiber systems in the tectum and basal zone. **b** Section at the medial mesencephalic level at E.40; the nerve fiber systems in the tectum and tegmentum are still weakly immunopositive. **c** Higher magnification of a section at the same level as in **a** at E.37 showing details of positive fine fibers in the tracts of the pretectal zone. **d** Note the intense immunostaining on the nervus oculomotorius (*III*), the commissura dorsalis tegmentalis (*cdt*) and of the *flm* at hatching. **e** Note the strong immunoreaction in the fibers of the trochlear nerve (*IV*) and of the *flm* at hatching

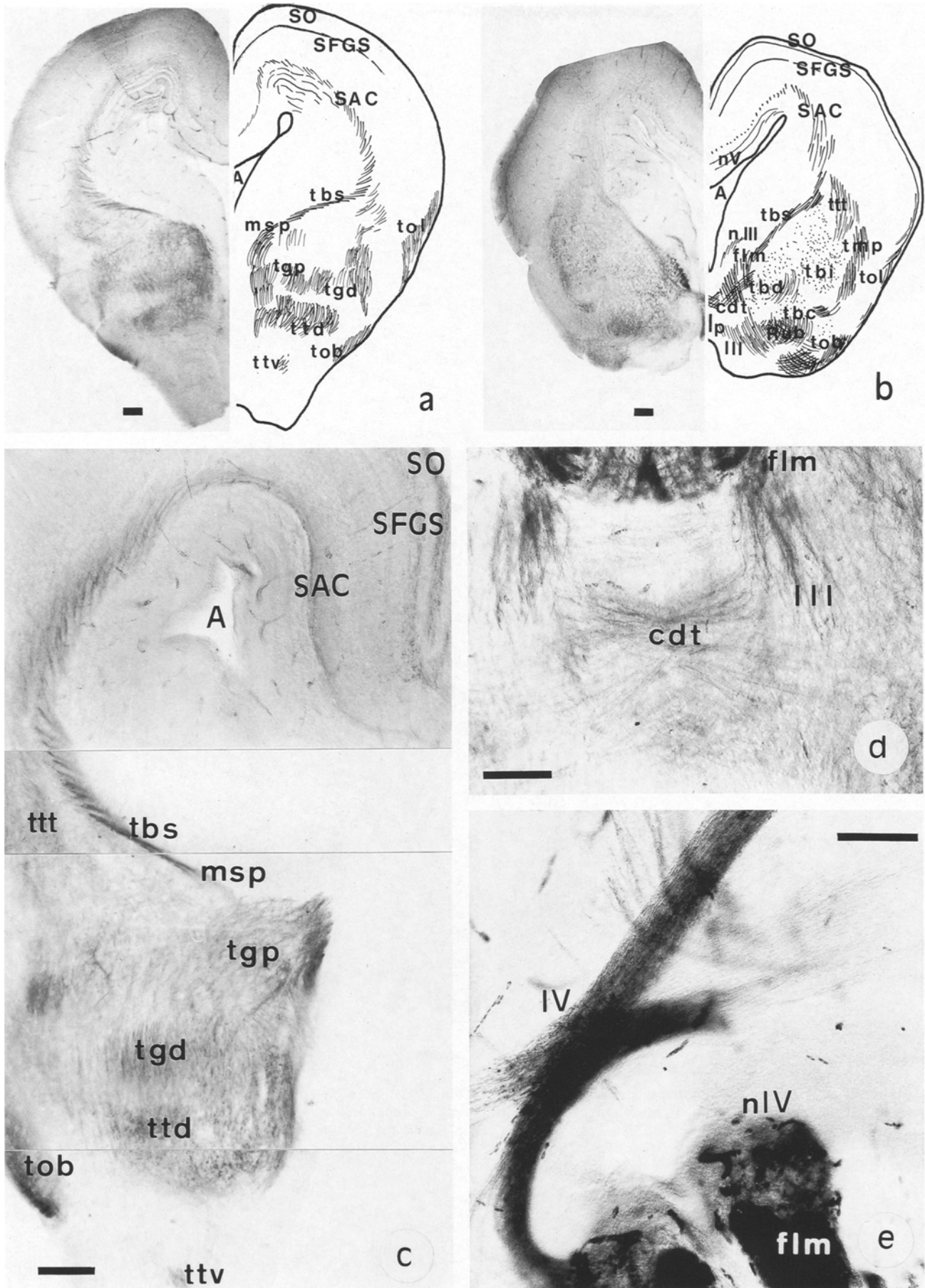
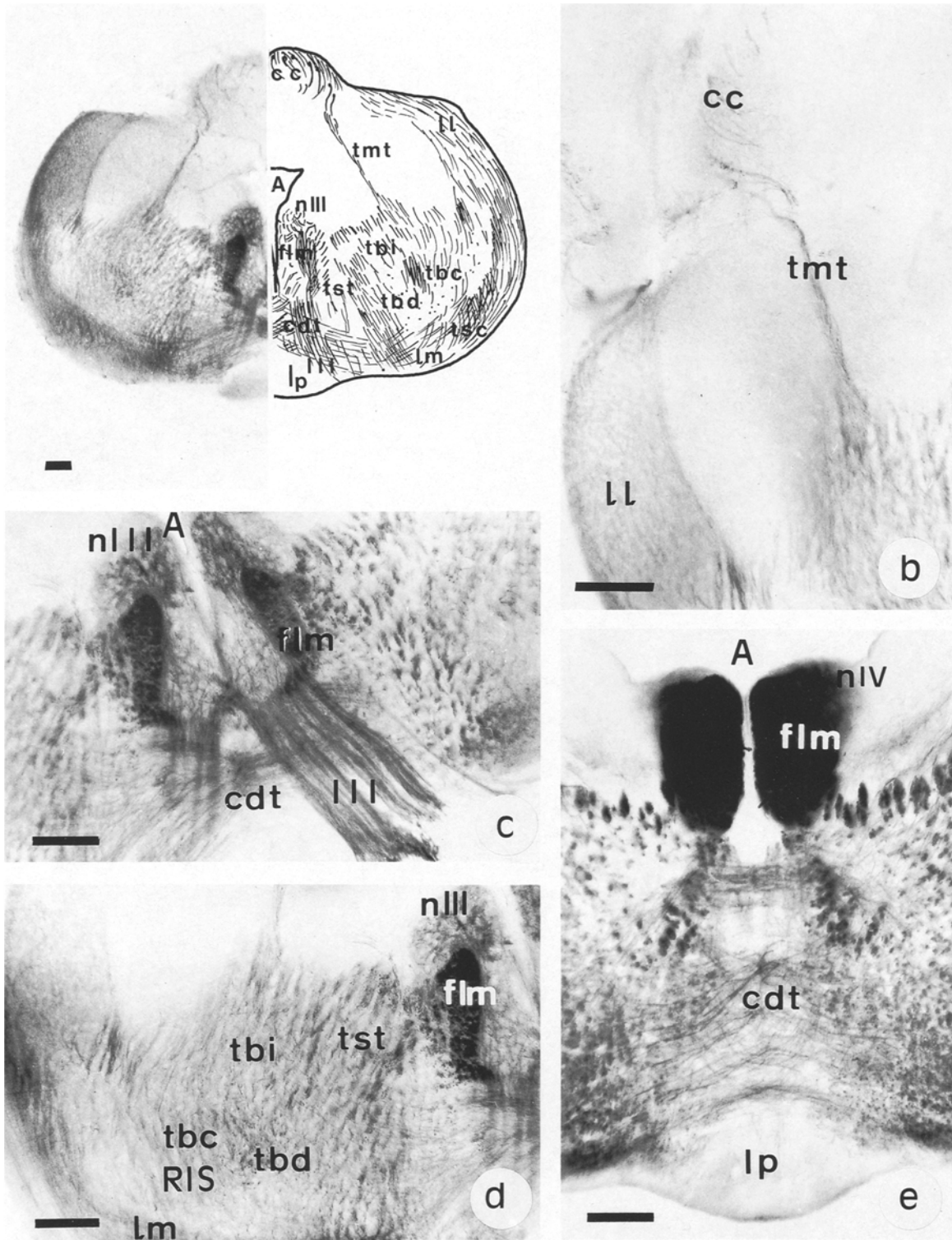


Fig. 7a-e



**Fig. 8a–e.** MBP-positive fibers (PAP method) in a caudal cross section of mesencephalon in a lizard at postnatal day 15. Bar 200 μm. **a** Overall view at low magnification. **b**, **c**, and **e** Details of the same or of contiguous tissue section(s) observed at higher magnification. Notice the intense immunostaining in the cross-sectioned *flm* (**a**, **c**, **d**, and **e**), *tbc*, *tbd*, *tbi*, *tsc* and *tst* (**a** and **d**). Other immunoreactive fibers coursing, at least partially, in the plane of the section are those of the *cc* and *tmt* (**a** and **b**), *lm* (**a** and **d**) and *cdt* (**a**, **c** and **e**)

tioned *flm* (**a**, **c**, **d**, and **e**), *tbc*, *tbd*, *tbi*, *tsc* and *tst* (**a** and **d**). Other immunoreactive fibers coursing, at least partially, in the plane of the section are those of the *cc* and *tmt* (**a** and **b**), *lm* (**a** and **d**) and *cdt* (**a**, **c** and **e**)

the oculomotor nerves and of the cdt (Fig. 8a, c), of the cc and the tmt (Fig. 8a, b) and of the tbc, tbd and tbi located laterally to the oculomotor nuclei (Fig. 8a, d).

## Discussion

MBP accounts for about 30% of the protein of mammalian CNS myelin (Kies et al. 1965; Eng et al. 1968). This protein has been thoroughly characterized (Mendel et al. 1978; Norton 1981) sequenced (Carnegie 1971 in man; Eylar et al. 1971 in cattle; Dunkley and Carnegie 1974 in rat) and cloned (Campagnoni 1988; Campagnoni et al. 1989). The protein appears first in *Elasmobranchia* and is present in all *Gnathostomata* (Wachneldt et al. 1986). Phylogenetic studies have shown that MBP forms of different molecular weight are present in different species, or can coexist in the same species, but all these MBP isoforms are recognized by the same antiserum (Marteson et al. 1971; Kerlero De Rosbo et al. 1984; Matthieu et al. 1986; Tai et al. 1986).

## Adult

Hartman et al. (1979), by using immunohistochemistry with an antiserum directed against MBP, determined that MBP in chick CNS is present only in areas corresponding to myelinated nerve fibers, and could not be detected in areas without myelinated fibers. MBP was also absent in the somata or dendrites of neurons, in astrocyte cell bodies or processes, and in microglia. By using the same approach we confirm here, with a strictly specific antiserum, that the same occurs in the lizard; we could follow the path of nerve fibers forming commissures and bundles in the lizard telencephalon and midbrain, and as far as we can judge all tracts and commissures that have been previously described in the literature are myelinated and MBP-immunopositive. Strikingly evident is the absence of *corpus callosum* which is a common feature of reptilian brain (Ariens-Kappers et al. 1965).

## Development

### *Onset of myelination*

In the rat, glial cell proliferation is very intense before the onset of myelination, and decreases during myelination (Bignami and Dahl 1973), while myelination of nerve fibers (Hartman et al. 1979) begins after axons have established their connections. Axon myelination is due to the presence of oligodendrocytes and oligodendroblasts along nerve tracts and fascicles. From these cells emerge the so-called trapezoid processes which wrap around the axons. It is the membrane of this process which undergoes biochemical transformation (including the incorporation of MBP) and becomes "myelin". In the rat, immunohistochemistry with anti-MBP antibodies has been used to monitor myelination. This

technique appeared to be more sensitive than the Weigert hematoxylin stain, and thus made it possible to detect myelin formation more precociously than with the classical histological techniques (Rozeik and Von Keyserlingk 1987).

Previous work (Yanes 1985; Yanes et al. 1987, 1989) has shown that, in *Gallotia galloti*, distinct nerve bundles emerging from the different nuclei begin to be distinguished at E.33 in telencephalon and E.32 in midbrain. By using immunohistochemistry with an antiserum directed against MBP we have established that myelination begins at E.40 in the lizard telencephalon, and at E.37 in midbrain. This coincides with the previously reported first appearance of active oligodendrocytes (Monzon-Mayor et al. 1990d).

In contrast to many reports in mammals, chick or amphibians, we never detected immunoreactive oligodendrocyte cell bodies in *Gallotia galloti* at any age. This result is at variance with the described presence of MBP immunoreactivity in the cell body and processes of mammalian oligodendrocytes during myelination (Sternberger et al. 1978a, b) although Bjelke and Seiger (1989) did not find MBP-positive oligodendrocytes in developing rat CNS. Many possible explanations are available: the simplest are at the technical level, for example the low amounts of MBP from the cell bodies could have been extracted by the ethanol-acetic acid permeabilization treatment of the sections; alternatively we can suppose an insufficient penetration of antibodies in the oligodendrocyte cytoplasm. Other explanations could depend on interspecific differences, such as a concentration of antigen in the lizard oligodendrocyte cell body much lower than in other myelinating animal species, and so low as to be below the threshold of detection by our method. Hartman et al. (1979) suggested that, in adults, MBP is not detectable in cell bodies because it is transported to the trapezoid processes at such a great velocity that all neosynthesized MBP is rapidly removed from the oligodendrocyte cell body as soon as it is synthesized. More recently it has been shown that mRNA coding for MBP is present in oligodendrocyte processes (Zeller et al. 1985) indicating the possibility of MBP synthesis occurring practically in loco following the transport of the messenger RNA and not of the transcription product. It is possible then that these transport processes are very active in this lizard. Finally we can suppose that the MBP present in the perinuclear region of rat myelinating oligodendrocytes consists of low molecular weight isoforms (so called SBP). In fact in our western blots we have not detected low molecular weight isoforms of lizard MBP which, thus, appear to be absent or more probably too minor to be detected in whole brain extracts. Complex in situ hybridization studies with probes of MBP mRNA on brain sections and in cultured cells in conjunction with the use of monoclonal antibodies specifically recognizing distinct epitopes present or absent in the different MBP isoforms are needed for choosing between the different possibilities.

We have also used an antibody directed against carbonic anhydrase II, an oligodendrocyte marker in mammals, but could not detect any immunoreaction, probab-

ly because of interspecific differences of the enzyme molecule (not shown).

### Regional chronology of myelination

During chick or rat development, the first fibers reacting with an anti-MPB immune serum are those located in the spinal cord, and the last are those localized in the cerebral cortex (Hartman et al. 1978). In the lizard, MBP appears at E.37 in the midbrain and at E.40 in telencephalon as a very weak immunoreactivity in the caudal level of the lateral bundle. This confirms our former morphological data (Yanes 1985). It appears then that, as in the chick and rat, the lizard myelination proceeds from the most caudal regions to the most rostral. Also at each level myelination proceeds from the ventral (or basal) to the dorsal (or alar) regions.

Myelination in the chick begins at incubation day 14, and is completed 2 or 3 days before hatching, while in mammals brain myelinogenesis is mainly postnatal, and is completed in the rat at the end of the 3rd postnatal week (Hartman et al. 1979; Bjelke and Seiger 1989). In lizards myelination begins at late prenatal stages and progresses after hatching at least until the 15th postnatal day.

### Myelination and astrocytes

As in the rat, the glial cell population in *Gallotia galloti* (Yanes et al. 1990; Monzon-Mayor et al. 1990a, b) increases noticeably before the beginning of myelination, and decreases in the post-hatching period when myelination is well advanced (Monzon-Mayor et al. 1990c, d; Yanes, unpublished results). Immunohistochemical experiments have shown that the increase involves astrocytes (Monzon-Mayor et al. 1990a, b; Yanes et al. 1990). At later ages abundant astrocytes are seen along the nerve fiber tracts. This was noticed by early authors who suggested a role for astrocytes in myelinogenesis. Also, electron microscopy has shown the presence of oligodendrocytes, astroblasts and astrocytes during myelination of bundles and commissures of lizard telencephalon (Yanes, unpublished results) and midbrain (Monzon-Mayor et al. 1990c, d). Bignami and Dahl (1973) suggested that in cerebral cortex the GFAP protein appears simultaneously with or just before the beginning of myelin formation. In our case, we have also observed that during the development of *Gallotia galloti* cerebrum the apparition of GFAP and of glutamine synthetase in glial cells and the formation of myelin in the same region are concomitant. Whether this is a simple coincidence or is the indication of a partnership between oligodendrocytes and astrocytes (or a class of astrocytes) in the process of myelination remains to be ascertained by future experiments.

**Abbreviations:** *A*, Aquaeductus (Cerebral Aqueduct); *ADVR*, Hyperstria anterior (anterior dorsal ventricular ridge); *av*, alveus; *Amc*, nucleus centralis amygdalae; *Aml*, nucleus lateralis amygdalae; *ca*, commissura anterior; *cc*, commissura colliculi; *ccp*, corpus quadrigeminus posterior; *cdt*, commissura dorsalis tegmentalis or decussatio tegmentalis; *Ch opt*, chiasma opticum; *cpa*, commissura

pallii anterior; *DC*, cortex dorsalis (dorsal cortex); *DMC*, cortex dorsomedialis (dorso medial cortex); *epl*, stratum plexyforme externum (external plexiform layer); *gl*, Stratum granulare (granular layer); *flm*, fasciculus longitudinalis medialis; *Ic*, nucleus isthmi, pars magnocellularis caudalis; *Ip*, nucleus interpeduncularis; *ipl*, stratum plexyforme internum (internal plexiform layer); *Isp*, nucleus isthmi, pars parvocellularis; *LC*, cortex lateralis (lateral cortex); *lfb*, tractus telencephalicus lateralis (lateral forebrain bundle); *ll*, lemniscus lateralis; *lm*, lemniscus medialis; *MC*, cortex medialis (medial cortex); *mfb*, tractus telencephalicus medialis (medial forebrain bundle); *mfp*, fasciculus mesencephalicus periventricularis (mesencephalic periventricular system); *nIII*, nucleus nervii oculomotorii (III nerve pair); *nIV*, nucleus nervii trochlearis (IV nerve pair); *nV*, nucleus nervii trigemini (V nerve pair); *NS*, nucleus sphaericus; *Nsa*, nucleus septalis anterior; *Nsd*, nucleus septalis dorsalis; *Nsl*, nucleus septalis lateralis; *Ntol*, nucleus tracti olfactorii lateralis; *Pr*, nucleus profundus mesencephali rostralis; *PT*, Pretectum (Pretectal zone); *RIS*, nucleus reticularis isthmi; *Rub*, nucleus ruber; *rM*, Radiations of Meynert; *SAC*, stratum album centrale; *SAP*, stratum album periventriculare; *SFGS*, stratum fibrosum et griseum superficiale; *SGC*, stratum griseum centrale; *SGP*, stratum griseum periventriculare; *SO*, stratum opticum; *stm*, stria medullaris; *Strv*, striatum ventralis; *tbc*, tractus tecto-bulbaris cruciatus; *tbd*, tractus tecto-bulbaris dorsalis rectus; *tbi*, tractus tecto-bulbaris intermedius rectus; *tbs*, tractus tecto-bulbo spinalis rectus; *tbv*, tractus tecto-bulbaris ventralis; *tgd*, tractus geniculatus descendens; *tgp*, tractus geniculatus pretectalis descendens; *tmp*, tractus mesencephalicus profundus; *tmt*, tractus mesencephalicus trigemini; *tob*, tractus nuclei opticus basalis; *tol*, tractus opticus lateralis; *toif*, tractus olfactorius; *tom*, tractus opticus marginalis; *tpoc*, tractus paraolfacto-corticalis; *TS*, torus semicircularis; *tsc*, tractus spino-cerebellaris; *tsh*, tractus septo-hypothalamicus; *tst*, tractus spino-thalamicus; *ttc*, tractus tecto-thalamicus dorso medialis anterior; *tti*, tractus tecto-isthmalis; *ttv*, tractus tecto-thalamicus ventrolateralis; *ttt*, tractus tecto-tegmentalis; *TZ*, Tegmentum (Tegmental zone); *III*, nervus oculomotorius (III nerve pair); *IV*, nervus trochlearis (IV nerve pair)

Abbreviations are from Ariens-Kappers (1965), Barbas-Henry and Lohman (1986), Huber and Crosby (1933a, b), Pérez-Clausell (1988), Smeets et al. (1986), Ten Donkelaar et al. (1984) and Yanes et al. (1987).

**Acknowledgements.** The authors wish to thank Professor Puelles Lopez for his helpful criticism of this manuscript. We are also indebted to Dr M.S. Ghandour for providing us with the immune serum, and to Mrs Y. Schladenhaufen for her skillful assistance. This work was carried out thanks to the support of the Spanish and French Ministries of Education (Action intégrée/integrada 1991 n° 173), of the University of Las Palmas de Gran Canaria (grant n° 145) and was partially supported by a DGICYT research grant (PB 87-0688 CO-02).

### References

- Ariens-Kappers CU, Huber GC, Crosby EC (1965) The comparative anatomy of the nervous system of vertebrates, including man. Hafner, New York
- Barbas-Henry HA, Lohman AHM (1986) The motor complex and primary projections of the trigeminal nerve in the monitor lizard, *Varanus exanthematicus*. *J Comp Neurol* 254:314–329
- Bignami A, Dahl D (1973) Differentiation of astrocytes in the cerebellar cortex and the pyramidal tracts of the newborn rat: an immunofluorescence study with antibodies to a protein specific to astrocytes. *Brain Res* 49:393–402
- Bischoff W (1982) Die innertriche Gliederung von *Gallotia galloti* (Dumeril D. Bibron, 1839) (Reptilia, Sauria: Lacertidae) Anf Tenriffa, Kanarische Inseln. *Bonn Zool Beitr* 33:363–381
- Bjelke B, Seiger A (1989) Morphological distribution of MBP-like immunoreactivity in the brain during development. *Int J Dev Neurosci* 7:145–164

- Campagnoni AT (1988) Molecular biology of myelin proteins from the central nervous system. *J Neurochem* 51:1–15
- Campagnoni AT, Roth HJ, Hunkeler M, Pretorius PJ, Campagnoni CW (1989) Expression of myelin basic protein genes in the developing mouse brain. In: Evrard P, Minkowski A (eds) *Developmental neurobiology, Nestlé nutrition workshop series*, Raven Press, New York, pp 95–109
- Carnegie PR (1971) Amino acid sequence of the encephalitogenic basic protein from human myelin. *Biochem J* 123:56–67
- Dufaure JP, Hubert J (1961) Table de développement du lézard vivipare (*Lacerta vivipara Jacquin*). *Arch Anat Microsc Morphol Exp* 50:309–327
- Dunkley PR, Carnegie PR (1974) Amino acid sequence of the smaller basic protein from rat brain myelin. *Biochem J* 141:243–255
- Eng LF, Chao FC, Gerstl B, Pratt D, Tavaststjerna MG (1968) The maturation of human white matter myelin. Fractionation of the myelin membrane proteins. *Biochemistry* 7:4455–4465
- Eng LF, Bigbee J (1978) Immunohistochemistry of nervous system specific antigens. In: Agranoff BW, Aprison MH (eds) *Advances in neurochemistry*, Plenum Press, New York, pp 43–98
- Eylar EH, Brostoff S, Hashim G, Caccam J, Burnett P (1971) Basic A1 protein of the myelin membrane. The complete amino acid sequence. *J Biol Chem* 246:5770–5784
- Ghandour MS, Langley OK, Clos J (1983) Immunohistochemical and biochemical approaches to the development of neuroglia in the CNS, with special reference to cerebellum. *Int J Dev Neurosci* 1:411–425
- Graham RC, Karnovsky MJ (1966) The early stages of absorption of injected horseradish peroxidase in the proximal tubules of the mouse kidney: ultrastructural cytochemistry by a new technique. *J Histochem Cytochem* 14:291–302
- Hartman BK, Agrawal HC, Kalmbach S, Shearer WT (1979) A comparative study of the immunohistochemical localization of basic protein to myelin and oligodendrocytes in rat and chicken brain. *J Comp Neurol* 188:273–290
- Huber GC, Crosby EC (1933a) The reptilian optic tectum. *J Comp Neurol* 57:57–163
- Huber GC, Crosby EC (1933b) A phylogenetic consideration of the optic tectum. *Proc Natl Acad Sci USA* 19:15–22
- Huber GC, Crosby EC (1934) The influence of afferent paths on the cytoarchitectonic structure of the submammalian optic tectum. *Psychiatr Neurol Bl Nos* 3 & 4:459
- Kerlero De Rosbo N, Carnegie PR, Bernard CCA, Linthicum DS (1984) Detection of various forms of brain myelin basic protein in vertebrates in electro-immunoblotting. *Neurochem Res* 9:1359–1369
- Kies MW, Thompson EB, Alvord EC Jr (1965) The relationship of myelin protein to experimental allergic encephalomyelitis. *Ann N Y Acad Sci* 122:148–161
- Marteson RE, Deibler GE, Kies MW (1971) The occurrence of two myelin basic proteins in the central nervous system of rodents in the suborders *Myomorpha* and *Sciuromorpha*. *J Neurochem* 18:2427–2433
- Matthieu JM, Widmer S, Herschkowitz N (1973) Biochemical changes in mouse brain composition during myelination. *Brain Res* 55:391–402
- Matthieu JM, Waehneltd TV, Eschmann N (1986) Myelin-associated glycoprotein and myelin basic protein are present in the central and peripheral nerve myelin throughout phylogeny. *Neurochem Int* 8:521–526
- Mendel JR, Whitaker JN (1978) Immunocytochemical studies of myelin basic protein. *J Cell Biol* 76:502–511
- Molowny A, Lopez C, Martin F (1972) Estudio citoarquitectónico de la corteza cerebral de reptiles. *Trab Inst Cajal Inv Biol L XIV*, 125–152
- Monzon-Mayor M, Yanes C, Tholey G, de Barry J, Gombos G (1990a) Immunohistochemical localization of glutamine synthetase in mesencephalon and telencephalon of the lizard *Gallotia galloti* during ontogeny. *Glia* 3:81–97
- Monzon-Mayor M, Yanes C, Ghandour MS, de Barry J, Gombos G (1990b) Glial fibrillary acidic protein and vimentin immunohistochemistry in the developing and adult midbrain of the lizard *Gallotia galloti*. *J Comp Neurol* 295:569–579
- Monzon-Mayor M, Yanes C, James JL, Sturrock RR (1990c) An ultrastructural study of the development of astrocytes in the midbrain of the lizard. *J Anat* 170:33–41
- Monzon-Mayor M, Yanes C, James JL, Sturrock RR (1990d) An ultrastructural study of the development of oligodendrocytes in the midbrain of the lizard. *J Anat* 170:43–49
- Norton WT (1981) Formation structure and biochemistry of myelin. In: Siegel GJ, Albers RW, Katzman R, Agranoff BW (eds), *Basic neurochemistry*. Little, Brown & Co, Boston, pp 63–92
- Nussbaum JL, Roussel G (1983) Immunocytochemical demonstration of the transport of myelin proteolipids through the Golgi apparatus. *Cell Tissue Res* 234:547–559
- Pérez-Clausell J (1988) Organization of Zinc-containing terminal field in the brain of the lizard *Podarcis hispanica*: histochemical study. *J Comp Neurol* 267:153–171
- Ramon y Cajal P (1896) Estructura del encefalo del camaleon. *Rev Trim Microsc* 1:46–82
- Ramos A (1980) Tabla de desarrollo embrionario de *Lacerta Galloti* (perodo de embriogenesis) y aspectos de su reproducción. Memoria de Licenciatura. Univ la Laguna. Tenerife. Canary Island, Spain
- Rozeik C, Von Keyserlingk D (1987) The sequence of myelination in the brainstem of the rat monitored by myelin basic protein immunohistochemistry. *Dev Brain Res* 35:183–190
- Smeets WJAJ, Hoogland PW, Lohman AHM (1986) A forebrain atlas of the lizard *Gekko gekko*. *J Comp Neurol* 254:1–19
- Sternberger LA, Hardy PH, Cuculis JJ, Meyer HG (1970) The unlabeled antibody-enzyme method of immunocytochemistry. Preparation and properties of soluble antigen antibody complex (HRP-antiHRP) and its use in identification of spirochetes. *J Histochem Cytochem* 18:315–333
- Sternberger NH, Itoyama Y, Kies MW, Webster H de F (1978a) Immunocytochemical method to identify basic protein in the myelin-forming oligodendrocytes of newborn rat CNS. *J Neurocytol* 7:251–263
- Sternberger NH, Itoyama Y, Kies MW, Webster H de F (1978b) Myelin basic protein demonstrated immunocytochemically in oligodendroglia prior to myelin sheath formation. *Proc Natl Acad Sci USA* 75:2521–2524
- Tai FL, Smith R, Bernard CCA, Hearn MWT (1986) Evolutionary divergence in the structure of myelin basic protein: comparison of Chondrichthye basic proteins with those of higher vertebrates. *J Neurochem* 46:1050–1057
- Ten Donkelaar HJ, R de Boer-van Huizen (1984) The fasciculus longitudinalis medialis in the lizard *Varanus exanthematicus*. Interstitio-spinal, reticulo-spinal and vestibulo-spinal component. *Anat Embryol* 169:177–184
- Waehneltd TV, Matthieu JM, Jeserich G (1986) Appearance of myelin protein during vertebrate evolution. *Neurochem Int* 9:463–474
- Yanes C (1985) Ontogenia de las áreas basales telencefálicas de *Gallotia galloti* (reptil Lacertidae). *Anuario Univ La Laguna* 2:11–66
- Yanes C, Pérez-Batista MA, Martín-Trujillo JM, Monzon-Mayor M, Marrero A (1987) Anterior dorsal ventricular ridge in the lizard: embryonic development. *J Morphol* 194:55–64
- Yanes C, Pérez-Batista MA, Martín-Trujillo JM, Monzon-Mayor M, Rodriguez A (1989) Development of the ventral striatum in the lizard *Gallotia galloti*. *J Anat* 164:92–100
- Yanes C, Monzon-Mayor M, Ghandour MS, de Barry J, Gombos G (1990) Radial glia and astrocytes in developing and adult telencephalon of the lizard *Gallotia galloti* as revealed by immunohistochemistry with anti-GFAP and anti-vimentin antibodies. *J Comp Neurol* 295:559–568
- Zeller NK, Behar TN, Dubois-Dalcq ME, Lazzarini RA (1985) The timely expression of myelin basic protein gene in cultured rat brain oligodendrocytes is independent of continuous neuronal influences. *J Neurosci* 5:2955–2962